ELSEVIER

Journal of Alloys and Compounds 271–273 (1998) 670–675

Journal of ALLOYS AND COMPOUNDS

Irradiation behavior of microspheres of U-Zr alloys

T. Ogawa[a,*], T. Ogata[b], A. Itoh[a], M. Akabori[a], H. Miyanishi[a], H. Sekino[a], M. Nishi[a], A. Ishikawa[a]

[a] *Japan Atomic Energy Research Institute, Tokai-mura, Naka-gun, Ibaraki-ken, 319-11, Japan*
[b] *Central Research Institute of Electric Power Industry, 11-1, Iwato Kita 2-Chome, Komae-shi, Tokyo, 201, Japan*

Abstract

In order to understand the fundamental behavior of metallic fuels, microspheres of U-Zr alloys were prepared and irradiated. The microspheres of about 0.8 mmϕ were formed by solidifying fused droplets of U-Zr alloys. Irradiation temperatures were controlled by external electric heating. Burnup reached 1.5 at%. After the irradiation, fractional release of fission-product gases, dimensional change and microstructure were examined. The results were compared with the analysis by a metal-fuel performance code ALFUS. © 1998 Elsevier Science S.A.

Keywords: UZr; Microspheres; Irradiation

1. Introduction

The U-Pu-Zr alloys are candidate fuels for the liquid–metal fast reactor. Its performance has been extensively studied in the Argonne National Laboratory [1]. The fuel performance codes with mechanistic modeling have been written, which describe the behavior of the metallic fuels along the line developed for the ceramic fuels [2–4]. However, some characteristics of the metallic fuels differ from the ceramic fuels. For instance, metals generally have a smaller ratio of grain-boundary energy to surface energy than ceramics. This fact would make the formation of grain-boundary tunnels by bubble interlinkage more difficult. Also there are factors such as the irradiation growth of crystals, which are normally absent in the ceramic fuels. In addition, a significant component redistribution in the U-Pu-Zr fuel slugs [1] makes it difficult to retrace the irradiation behavior of the alloys as a function of local irradiation conditions from the evidences of the post-irradiation examination.

To better understand the behavior of the metallic fuels, microspheres of U-Zr alloys were irradiated. The temperature was controlled by external heating. The irradiation was made in a condition of virtual absence of the external mechanical constraint. Although this condition was different from that in the actual fuel element, the test gave fundamental information on the bubble behavior in the alloy matrix. The results were compared with the prediction by a metal fuel performance code ALFUS [2].

2. Experimental

2.1. Sample preparation

Metal uranium of 19.4 wt% enrichment was alloyed with crystal-bar zirconium by arc-melting. Microspheres of about 0.4–1.0 mmϕ were formed by dropping fused alloys (10, 30 and 70 at% Zr) through a Y_2O_3 ceramic orifice of 0.3 mm diameter. Induction heating was made with a tungsten suscepter. The droplets were solidified while falling in a helium-filled jacket of about 1.5 m height, which was connected to a cooled copper hearth. Each microsphere was loosely wrapped with a zirconium foil with an inner diameter of about 2 mm, and sealed with a quartz wool in a quartz tube of 6 mm OD×4 mm ID×26 mm length. While the tube was evacuated to 10^{-3}Pa, the quartz wool was degassed at 200°C. Then the tube was sealed under helium at 0.02 MPa. Oxygen content in helium was kept less than 10 ppm.

2.2. Sample characterization

A cross-section of an as-cast microsphere (nominal zirconium content of 30.0 at% or 14.1 wt%) is shown in

*Corresponding author. Tel.: 29-282-5430; fax: 29-282-6097; e-mail: ogawa@SUN2SARL.tokai.jaeri.go.jp

0925-8388/98/$19.00 © 1998 Elsevier Science S.A. All rights reserved.
PII: S0925-8388(98)00184-4

Fig. 1a. The microstructure was rather featureless. The concentration fluctuated a little in 2–3-μm range, but was nearly homogeneous when analyzed over a 20–30-μm range. The matrix contained sparse inclusions of a Zr-rich phase, probably due to preferential segregation of the Zr(O) phase combined with impurity oxygen. In the surface area of less than one micron thickness, zirconium was concentrated to 23 wt% in comparison to the bulk (13.46±0.16 wt%). Within-batch particle-to-particle composition variation was small (<±0.2 wt% Zr).

Effects of high-temperature heating on the microsphere were studied. The U-30 at% microspheres sealed in the manner as described above were heated at 1073 K for 72 h and furnace cooled. The microstructure showed a typical two-phase structure (Fig. 1b). Although each phase was too minute for quantitative analysis, the alloy is considered to consist of α-U and δ-UZr_2. Concentration of zirconium in the surface scale increased to 46 wt%. Additional impurities, silicon and iron, were detected in the scale with concentrations of 0.2 and 0.4 wt%, respectively. Iron is considered to have originated from the zirconium wrapping; silicon from the quartz wool. From this observation the maximum irradiation temperature of 973 K was chosen.

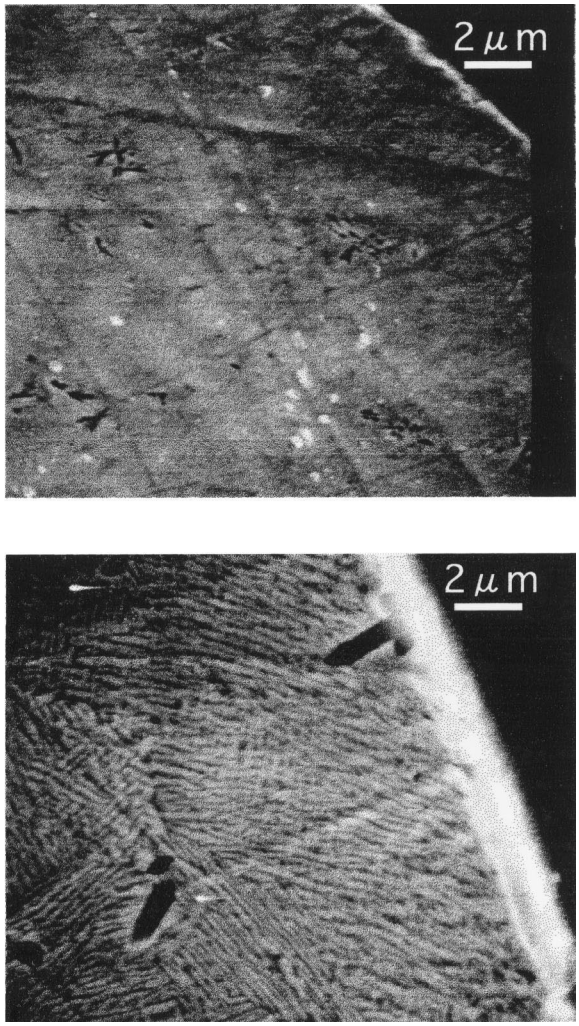

Fig. 1. Secondary electron image of the cross-sections of U-30 at% Zr microspheres. (a) As-cast microsphere, and (b) microsphere annealed at 1073 K for 72 h.

2.3. Irradiation and post-irradiation examinations

Six quartz capsules were loaded into a sample holder made of Type 304 steel. The irradiation capsule consisted of three sample holders, each of which was equipped with a resistance heater. The sample holders were controlled at nominal temperatures of 723, 873 and 973 K throughout the irradiation. The temperatures were measured by a thermocouple inside the wall of the sample holder. Maximum burnup reached 1.5 at% of uranium with 63 full power days in the research reactor JRR-2, JAERI. After the irradiation, quartz capsules were crushed, and fission-product gases were collected into a calibrated ionization chamber. It was found that the microspheres irradiated at 973 K had reacted severely with the zirconium foil. Those samples were rejected from further examinations. The result of the analysis by the ionization chamber was further checked by calibrated gamma spectrometry. Due to a long cooling period of 690 days, the radioactivity of gases was ascribed almost exclusively to ^{85}Kr. Dimensions of microspheres were measured before and after irradiation by X-ray microradiography, and corrected with the identical stainless-steel microsphere standards for the difference of measurement geometries and the film shrinkage. Some microspheres were polished to slightly below the equator, and then observed by an optical microscopy and an electron-probe microanalyzer. Quantitative analysis was made at an acceleration voltage of 25 kV.

3. Results of postirradiation examinations

3.1. Dimensional change and fission-gas release

The volumetric swelling [$\Delta V/V$(%)] and the fractional fission-gas release [FR(%)] are summarized in Table 1. The table gives estimated center temperatures (T_c) of microspheres. Each microsphere is estimated to have had a temperature gradient of about 15 K from the center to the surface. Additional temperature gaps between the sample surface and the bulk of sample holder were taken into account. The errors in $\Delta V/V$ originated from the deviation from the sphericity, which is not greater than 1.01 for U-30 at% Zr and U-70 at% Zr microspheres, and 1.02 for U-10 at% Zr microspheres, respectively, and also from the surface roughening by irradiation. Total errors, which also include those of the diameter reading on the microradiographs, are considered ±8% in $\Delta V/V$(%). Only U-10 at% Zr microsphere irradiated at 903 K showed an anisotropic

Table 1
Summary of irradiation test results

Position	% FIMA[a]	Sample	Zr (%)	FR (%)	$\Delta V/V$ (%)
Top T_c~743 K	1.3	Zr12	30	7.7	40
		Zr14	30	7.2	46
		Zr6	10	9.7	61
Bottom T_c~903 K	1.2	Zr7	30	12.5	67
		Zr10	30	10.5	42
		Zr5	10	15.7	[b]
		Zr1	70	0.02	3

The volumetric swelling [$\Delta V/V$(%)] has an error limit of ±8% $\Delta V/V$.
[a] Percent fissions per initial uranium atom.
[b] Deformation was too large.

large deformation, and $\Delta V/V$(%) was not calculated for this particular sample.

3.2. Microstructure

Optical micrographs of U-30 at% Zr microspheres are shown in Fig. 2. There was little difference in the microstructure between the center and surface regions of a given particle. The cross-sections developed pronounced etching by leaving in air; Fig. 2 gives pictures taken within the day of the final polishing. Larger bubbles were evident, but finer bubbles were difficult to distinguish due to smearing of the soft metal matrix during polishing and staining by air. Nevertheless the existence of submicron bubbles, where their number density is relatively large, was inferred from the foggy contrasts in the matrix area. Bubbles and pores, which were clearly discernible on the metallograph, account for 20–25% of the cross-section of the microspheres irradiated at 743 and 903 K.

Finer pores became much less noticeable in secondary and back-scattered electron images due to poorer contrast and absence of well-defined edges (Fig. 3). Distribution of U-rich and Zr-rich phases changed from those before irradiation shown in Fig. 1. It was identified that the U-rich phase (1.7 at% Zr) was α-U, and the Zr-rich phase (61 at% Zr) was a (γ-U,β-Zr) solid solution at 903 K, in good agreement with the binary phase diagram. For the microsphere irradiated at 743 K, the (γ-U,β-Zr) phase would have been replaced by the δ-UZr_2 phase.

There was no apparent bubble interlinkage along the boundaries between α-U and (γ-U,β-Zr) regions for the microsphere irradiated at 903 K. Larger bubbles seemed preferentially associated with (γ-U,β-Zr), but there was no apparent tendency of linking between adjacent bubbles. On the other hand, for the microsphere irradiated at 743 K, where a fine lath-like microstructure is still retained, a tendency of network formation among bubbles was noted. Elongated bubbles of a few μm thickness formed a vague pattern of network with a mesh size of 10–30 μm. The mesh size of this network is, however, much larger than the size (a few-micron thick) of each phase.

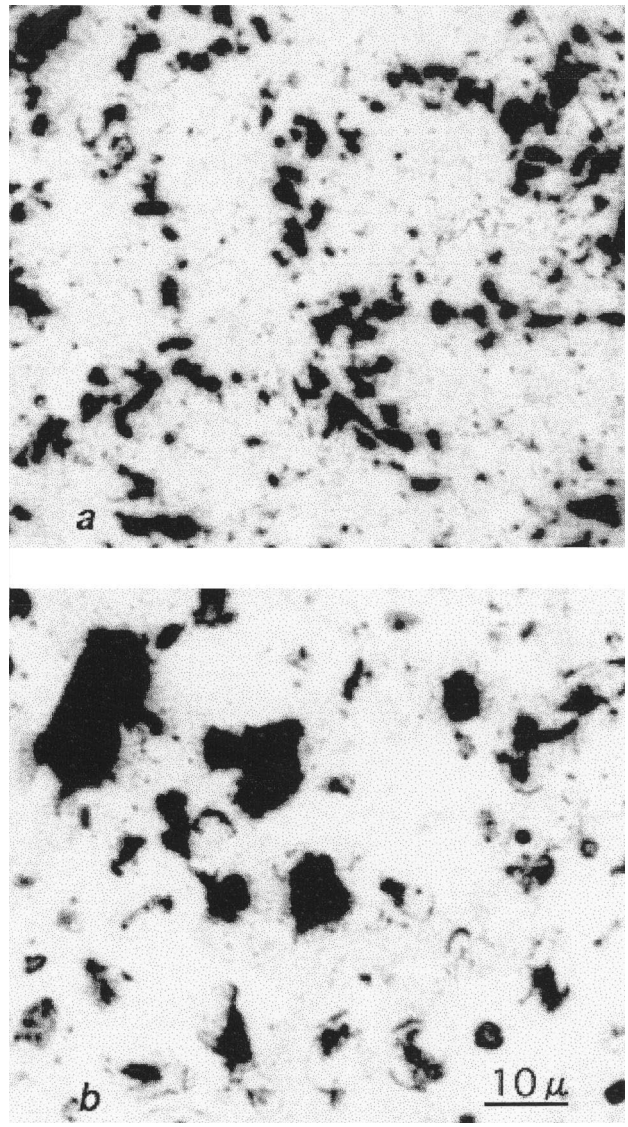

Fig. 2. Optical micrographs of irradiated U-30 at% Zr microspheres. (a) 743 K, (b) 903 K. (Electronically enlarged by 300% from the photographs at ×400).

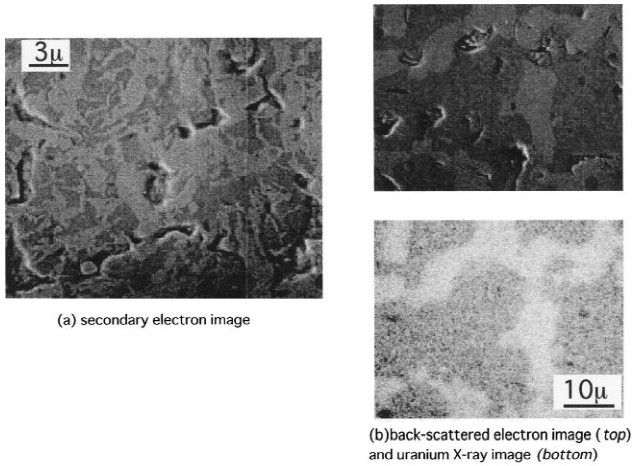

Fig. 3. Electron and characteristic uranium X-ray images of cross sections of U-30 at% Zr microspheres. (a) Secondary electron image of microsphere irradiated at 743 K; (b) back-scattered electron image and U X-ray image of microsphere irradiated at 903 K.

4. Comparison with simulation by ALFUS code

4.1. Analytical model

Simulations have been carried out by a computer code ALFUS [2]. The detailed description of the modeling is given elsewhere [2]. The analytical model for bubble growth is based upon the collision and coalescence among the bubbles due to their random motion. The bubbles are categorized into six classes (0 to 5) by the amount of gases in each bubble. Bubbles are assumed to be spherical, and their radii are determined by the van der Waals' equation of state equilibrated with the surface tension and the external stress. When total gas-bubble volume reaches a certain level, the open pore formation is calculated. The gas release is assumed to occur when the open pore is formed, or when the gas atoms or the gas bubbles collide with the open pores. The open pore is assumed to be compressible.

Since the parameters in the ALFUS have been tuned to the U-23 at% Zr-fuel behavior irradiated in the EBR-II, the simulations have been carried out for the comparable U-30 at% Zr specimens. The previous irradiation data showed that there were no appreciable differences in the irradiation behavior of U-Pu-Zr alloys for the composition ranges of 15–30 at% Zr [5]. Because spherical geometry is not readily treated in the cylindrical 2-dimensional finite-element calculation of the ALFUS, the microsphere was replaced by a cylindrical piece of 1 mm diameter. Burnup rate, temperature and initial pressure in the quartz capsule were the same as the experimental conditions.

The ALFUS code also includes the simplified tearing model to describe the anisotropic deformation of the cylindrical fuel slug due to crack or cavitation at the grain or phase boundaries. The pores corresponding to the tearing strain are treated as the open pores [2]. In these simulations, isotropic tearing strain (12 $\Delta V/V$%/at%-burnup) was assumed because the microstructure of the microsphere specimens appeared more isotropic than the cylindrical fuel slug.

4.2. Results of code simulation

Calculated volume changes of the U-Zr alloy are shown in Figs. 4 and 5. The 'large bubble swelling' in the figures denotes swelling due to bubbles of more than a micrometer size: $\Delta V/V$ (large bubble swelling)=25–33% from the fractional area (20–25%) of large bubbles in the metallographic cross section. The large bubble swelling for the

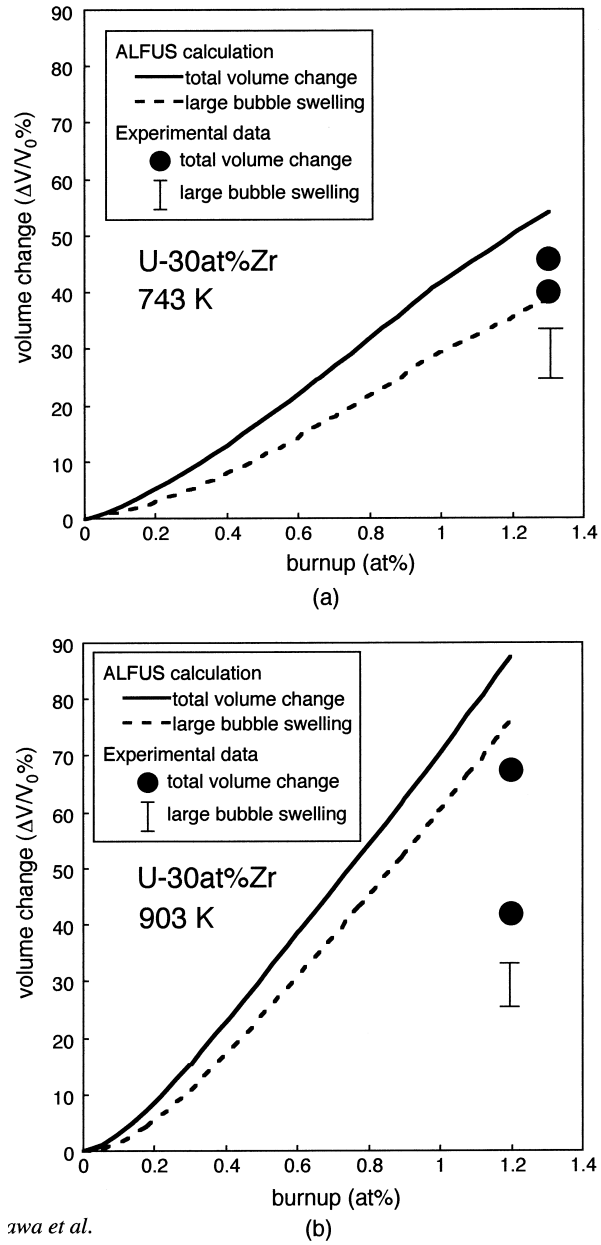

Fig. 4. Prediction by ALFUS code: Swelling of U-30 at% Zr microspheres irradiated at (a) 743 K and (b) 903 K.

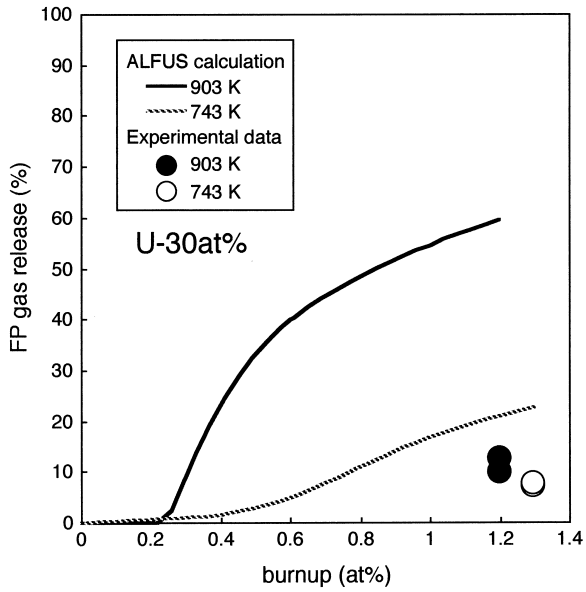

Fig. 5. Prediction by ALFUS code: Fractional release of fission-product gas atoms.

ALFUS calculation corresponds to that due to the 5th class closed-bubbles and the open pores. In the case of the thicker fuel slug, such as the EBR-II fuel, radial distributions of swelling rate and thermal expansion cause compressive stress in the inner region of the slug, which decreases open-pore volume even before the slug-cladding gap closure. In the spherical or equivalent cylindrical specimen of the smaller diameter, however, decrease of the open-pore volume is not significant because temperature and swelling rate are essentially uniform throughout the specimen.

Fig. 4(b) for 903 K shows: Calculated total swelling amounts to 90% of preirradiation volume at 1.2 at% burnup, and approximately 90% of this volume change is due to the large bubble swelling. The open pores contribute about $\Delta V/V=70\%$. As for the experimental data, swelling for 903 K is less than 70%, and the large bubble swelling is about half of the total volume change. Besides, the open pore formation was not evident in the metallographs. The ALFUS also slightly overestimates the total volume change and the large bubble swelling at 743 K, as shown in Fig. 4(a). These discrepancies mean that contribution of the smaller bubbles to the total volume change is more significant than that predicted by ALFUS.

In the case of the EBR-II test fuel of 75% smear density, the cylindrical fuel slug swells to approximately 45% and releases more than 40% of fission gas generated by the time of fuel-cladding gap closure [6]. To reproduce this behavior, the ALFUS model assumes that the open-pore formation starts after swelling of 10%, which leads to higher level of the gas release, as shown in Fig. 5. The measured data showed less than 13% gas release for both at 903 and 743 K, although swelling of 40 to 60% was observed.

5. Discussions

The fractional gas release for U-30 at% Zr microspheres were less than the ALFUS calculations. The discrepancy is hardly explained by the possible difference of the properties between U-23 at% Zr, to which the code was tuned, and the U-30 at% alloys. Even if the bubble mobility in the calculation was reduced by 40%, the agreement does not improve appreciably. This discrepancy may be attributed rather to a possible mechanism of the bubble interconnection in the thick cylindrical geometry of EBR-II fuel element. The internal stress causes cracking in the alloy matrix more readily in the cylindrical slug-type fuel. The bubble interconnection will be promoted by the cracking. Constraint by the cladding will also affect the stress state in the slug. The microspheres in this study, however, would have been relatively free from the irradiation-induced stresses, and they would have swelled with less mechanical constraint.

The experimental volume change components due to the smaller bubbles at 903 K were larger than those predicted by ALFUS. This suggests that growth rate of gas bubbles is slower than the calculation. In the ALFUS code, the bubble growth rate depends on migration rate of gas atoms into bubbles and collision-coalescence rate among bubbles. The mobilities of gas atoms and bubbles have been adjusted so as to reproduce experimental data of the fuel irradiated in the fast reactor, EBR-II. The mobilities under thermal neutron field, however, may differ from those in the fast reactor.

There are also features of U-Zr alloys which have not been incorporated in the simulation code. The experimental results showed:

The grain boundary, which has an important role in ceramic fuels, has less significance in the formation and development of bubbles in U-Zr alloy fuels, at least in the absence of substantial mechanical constraint.

It seems important to take into account the essential heterogeneity of the alloys: U-Zr alloys consist of two phases at normal operating temperatures. Physical properties of U-rich and Zr-rich phases significantly differ from each other. In addition, the Zr-rich phase transforms between hexagonal δ and a bcc solid solution (γ-U,β-Zr), and accordingly its physical properties change at about 880 K [7,8].

Also the gas generation rate itself is not uniform in the alloys.

These characteristics of the U-Zr alloys may be also responsible for the discrepancy between the prediction and the experimental results, particularly at 903 K, where the

fuel matrix consisted of coarse grains of α-U and (γ-U,β-Zr).

6. Conclusion

Microspheres of U-Zr alloys were prepared and irradiated. After the irradiation, fractional release of fission-product gases, dimensional change and microstructure were examined. The results were compared with the analysis by a metal fuel performance code ALFUS. Characteristic features of U-Zr alloys, which are different from the past hypotheses in analyzing its irradiation behavior, were identified.

References

[1] R.G. Pahl. et al. Proc. Intern. Fast Reactor Safety Mtg. Snowbird, Utah, vol. 4, 1990, pp. 129–137
[2] T. Ogata, et al., J. Nucl. Mater. 230 (1996) 129.
[3] W.G. Steele, et al., Nucl. Eng. Des. 113 (1989) 289.
[4] M.C. Billone et al. Proc. Intern. Conf. on Reliable Fuels for Liquid Metal Reactors, Tucson, Arizona, Sep. 7-11, 1986, pp. 5.77–5.92.
[5] H. Tsai et al. The 3rd JSME/ASME Joint Int. Conf. on Nucl. Eng. (ICONE-3), 1995, Kyoto, Japan.
[6] R.G. Pahl, et al., Metallurg. Transact. A 21A (1990) 1893.
[7] M. Akabori, J. Phys.: Condens. Matter 7 (1995) 8249.
[8] M. Akabori et al. J. Nucl. Mater. (in press).